Electrochimica Acta 379 (2021) 138029

Contents lists available at ScienceDirect

Electrochimica Acta

journal homepage: www.elsevier.com/locate/electacta

Theory of transport and recovery in microbial electrosynthesis of acetate from CO_2

J.E. Dykstra[a,*], A. ter Heijne[a], S. Puig[b], P.M. Biesheuvel[c]

[a] Environmental Technology, Wageningen University, Bornse Weilanden 9, 6708 WG Wageningen, The Netherlands
[b] Laboratory of Chemical and Environmental Engineering (LEQUiA), Institute of the Environment, University of Girona, Carrer Maria Aurèlia Capmany, 69, E-17003 Girona, Spain
[c] Wetsus, European Centre of Excellence for Sustainable Water Technology, Oostergoweg 9, 8911 MA Leeuwarden, The Netherlands

ARTICLE INFO

Article history:
Received 6 January 2021
Revised 16 February 2021
Accepted 19 February 2021
Available online 26 February 2021

Keywords:
Bio-electrochemical systems
Multi-component mass transport
Amphoteric ions
Ion exchange membranes
Bipolar membranes

ABSTRACT

Microbial electrosynthesis (MES) provides a sustainable route for the conversion of CO_2 and electricity into acetate and other organics. The conversion of CO_2 takes place at a biologically active cathode ('biocathode'), which is typically separated from the anode by an ion exchange membrane. Since both charged and uncharged species participate in the reaction, understanding the transport of these species through the membrane, and how this depends on the type of membrane, is of key importance. We develop a theory for ion mass transport and conversion in these types of microbial electrochemical cells. The theory includes ion transport, acid-base reactions, as well as electrochemical reactions at the electrodes. We first analyze a cell configuration including three compartments, in which the acetate recovery compartment in the middle is separated from the outer compartments by one cation exchange membrane and one anion exchange membrane, and we compare with experimental data from literature. Analysis of ion transport across the ion exchange membranes revealed that acetic acid/acetate and carbonic acid/bicarbonate species were used as proton shuttles between the catholyte compartment and the recovery compartment. We also analyzed a system including a bipolar membrane (BPM). Our results showed that a commonly made assumption that in BPMs the charge is solely carried by protons and hydroxyl ions, produced inside the BPM, is not generally correct. In our calculation charge is mainly carried by protons in the cation exchange layer of the BPM, while bisulphate and sulphate ions carry the charge in the anion exchange layer. In conclusion, we show that the ions which participate in acid-base reactions have to be considered in detail to describe and explain ion transport in MES cells and in the elements thereof such as BPMs.

1. Introduction

Microbial electrosynthesis (MES) provides a sustainable route for the conversion of electricity and CO_2 into acetate or other organic molecules [1,2]. In acetate-producing MES systems, electroactive microorganisms (acetogens) that are in the vicinity of an electrode take up hydrogen or electricity, and produce acetate from CO_2. At the anode, electrons are usually derived from water oxidation (see Fig. 1).

MES is a relatively new topic in the field of Microbial Electrochemical Technologies. Several studies on MES have shown an improvement in acetate production rates and have led to increased understanding of the factors that influence acetate production, such as the type of membrane [3,4], the cathode material [5,6], and operational conditions such as pH and cathode potential [7–9]. Most MES reactors consist of two compartments that are separated by a cation exchange membrane (CEM). Other membranes, such as anion exchange membranes (AEM) and bipolar membranes (BPM), have also been studied. Furthermore, a three-compartment configuration, with an extraction compartment between anode and cathode, has been demonstrated [3]. Ion transport through these different membranes, and its effect on MES performance, is still a topic under active investigation.

Both charged and uncharged ions play a role in the conversions at the electrodes, and we must understand their transport through different membranes. Improved theoretical understanding of transport of ions in MES systems helps to understand, improve and control MES performance.

* Corresponding author.
E-mail address: jouke.dykstra@wur.nl (J.E. Dykstra).

https://doi.org/10.1016/j.electacta.2021.138029

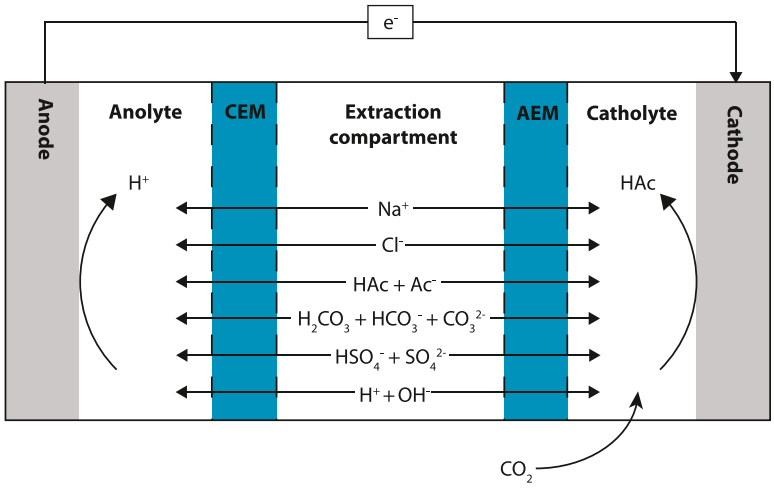

Fig. 1. Schematic view of ion transport and electrochemical reactions in one example configuration of a microbial electrosynthesis cell.

To date, there are only few modeling studies on MES. A comprehensive overview of the different parts of the system, and modeling strategies, is given by Korth and Harnisch [10]. Matemadombo et al. [11] combine an experimental approach with a modeling study to analyze and describe the acetate production rates and transport across the anion exchange membrane as a function of time. However, the transport of ions other than acetate, across different types of ion exchange membranes, and the effect of pH on the dissociation of amphoteric species such as acetate and carbonate, was not yet addressed.

We present a system-level theory for microbial electrosynthesis that includes electrochemical reactions at the electrodes and ion transport across the membranes to study the transport of the most prominent anions and cations in combination with acid-base reactions, see Fig. 1. This theory builds on previous work in which one dimensional steady-state theory was used to describe ion transport as a function of concentration and potential gradients in (bio)electrochemical systems and bioanodes [12–14]. In this approach infinitely fast acid-base reactions are assumed, which makes numerical analysis much easier compared to other models that include finite rates of the acid-base reactions.

In the present work, we further develop this approach to enable dynamic analysis of the processes in microbial electrosynthesis, including the theoretical analysis of production, extraction, and concentration of acetic acid [3,4].

We consider several cell configurations to illustrate our theory. In one specific configuration the extraction compartment is situated in the middle of the electrochemical cell, separated from the anolyte compartment by a cation exchange membrane (CEM), and separated from the catholyte compartment by an anion exchange membrane (AEM), see Fig. 1. Acetate produced at the cathode was transported (mainly driven by a potential gradient) from catholyte to extraction compartment, where it is concentrated in the form of acetic acid.

In the other example we describe a two compartment cell with either a cation exchange membrane or a bipolar membrane [4]. The three compartment system resulted in higher acetate concentrations compared to the two compartment systems, and it was found that HCO_3^- contributed considerably to charge balancing.

To show the relevance of our theoretical framework, we compare the experimental results [3,4] with our system-level theory for microbial electrosynthesis. In addition, we demonstrate the effect of different experimental conditions and membranes on ion transport and acetate production rates. Lastly, we present theory to describe the dynamic transport of amphoteric ions across bipolar membranes (BPMs). We include the formation of H^+ and OH^- as a means to 'carry the current' [15–18], which we combine with simultaneous flow of other ions that contribute to charge transport in the BPM, such as HSO_4^- and SO_4^{2-} [19].

Our theoretical model and its description of data serves as an example of how suitable models for ion transport and acid-base reactions, both in solution and for the electrochemical reactions at electrodes, leads to more understanding of bioelectrochemical systems, for instance microbial electrosynthesis of acetate from CO_2.

2. Theory

In this section, we present a theoretical framework of an electrochemical cell for microbial electrosynthesis. The first example is a three-compartment cell that combines acetate extraction and concentration. The system consists of the anolyte chamber, an extraction chamber (EC), and the catholyte chamber, with a cation-exchange membrane (CEM) between anolyte and EC, and an anion-exchange membrane (AEM) between EC and catholyte, in line with the configuration presented by Gildemyn et al. [3] and shown in Fig. 1. At the anode, water is converted to oxygen gas and protons; at the cathode dissolved CO_2 is converted to acetate. Acetate is expected to transport to the middle, extraction, chamber and collected there. The theory self-consistently predicts the fluxes of all ions and the pH-profiles that develop over time (dynamically) in the system, by combing electrode reactions, mass balances, and equations for ion transport through the membranes (including the effect of membrane charge). One relevant element in the theory is that to describe all acid-base reactions between all ions, we use a methodology used before in Dykstra et al. [12], Paz-Garcia et al. [13], de Lichtervelde et al. [14], Hwang and Helfferich [20], Hall et al. [21], Oren and Biesheuvel [22], Ronen et al. [23], Saville and Palusinski [24], Biesheuvel et al. [25].

This method, that assumes local chemical equilibrium for all acid-base reactions, simplifies the mathematics to a large degree, and needs much less kinetic information (information that often is not available). In the theoretical calculations that we present, of each species all possible protonation degrees are considered (such as both HAc and Ac^-) and their acid-base equilibria.

In any electrochemical cell, the applied (or, generated) current is directly connected to the reaction rates both on the anode and on the cathode, and these relate to the ionic current in the system. The stoichiometry of the electrode reactions, together with the

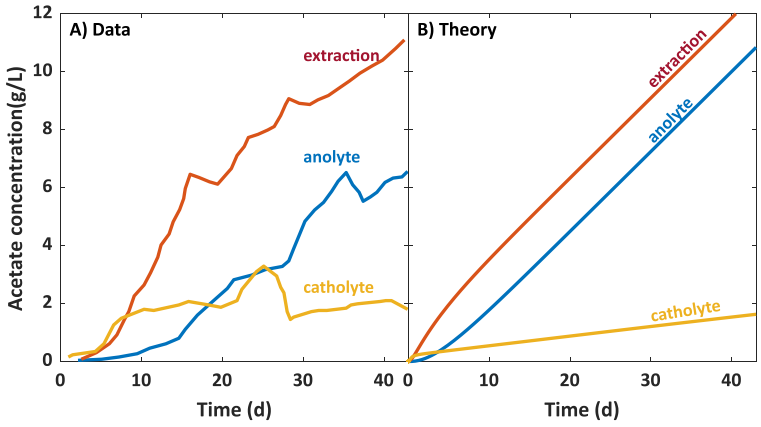

Fig. 2. Data and theory of acetate concentration as function of time in the extraction, anolyte and catholyte chamber for a 43 day experiment in the 3-compartment electrosynthesis cell depicted in Fig. 1. Data from Gildemyn et al. [3].

selectivities imposed by the membranes, determine the ionic fluxes, protonation degrees of all acid-base species, and changes in pH.

We make an example calculation based on Gildemyn et al. [3] and we simplify this system by considering of all ions only:

- the carbonic acid ions (H_2CO_3, HCO_3^-, and CO_3^{2-});
- the sulphate ions (SO_4^{2-} and HSO_4^-);
- the acetic acid (HAc) and acetate ion (Ac^-);
- the Na^+ ion (representing a summation of all monovalent cations);
- the Cl^- ion;
- the hydronium and hydroxyl ions (H_3O^+ and OH^-).

We will use the assumption of local chemical equilibrium for all groups of ions, thus for HAc $\Longleftrightarrow$ Ac^-, for H_2O $\Longleftrightarrow$ OH^- + H^+, for H_2CO_3 $\Longleftrightarrow$ HCO_3^- $\Longleftrightarrow$ CO_3^{2-}, and for SO_4^{2-} $\Longleftrightarrow$ HSO_4^-. We neglect all divalent cations, and we also neglect phosphate, and ammonium and ammonia, to reduce the number of equations. Nevertheless, the correspondence between our theoretical calculations and experimental results shown in Fig. 2, supports that our theory is adequate. However, for a precise comparison of theory with experimental data, these ions, in particular the phosphate species, must be included in the evaluation.[1]

A key element of the theory is the description of transport in the two ion-exchange membranes (IEMs) in the system. Here we focus on modeling a membrane of a single charge sign (AEM or CEM). As we will explain later on, a bipolar membrane (BPM) can be theoretically described as an AEM and CEM in direct contact, with a layer of vanishingly small thickness in between. IEMs are characterized by their fixed membrane charge density which leads to selective transport, where counterion transport is enhanced, and transport of co-ions hindered. Counterions are ions with a charge sign opposite to that of the membrane fixed charge groups, while co-ions have the same charge sign as the membrane. We can distinguish between an anion-exchange membrane (AEM), where anions are the counterions, and a cation-exchange membrane (CEM), where cations are the counterions. The transport of uncharged species is not directly influenced by the charge of the membrane, and they are transported through the membrane by diffusional forces only, neither accelerated nor retarded by the electrical field.

The theory that we use based on a full description of all ion fluxes and infinitely fast acid-base reactions in solution, has, amongst others, the following consequences that we discuss in detail later. In the theory we use, there is *no need to*

- set up balances in the ions H^+ or OH^-,
- describe the fluxes of H^+ or OH^- through the membranes,
- explicitly describe the participation of H^+ and OH^- at the two electrodes.

Indeed, at the electrodes, we do not need to define whether H^+ or OH^- takes part in a certain electrode reaction (which often is unknown and undefined). Instead, the theory will *predict* what are the fluxes of H^+ and OH^- into/out of each electrode.

In the present work, we do not describe the electroactive biofilm on the electrodes. Such a model, as reported in [14], helps to identify the reaction overpotential (relevant for a calculation of the total cell voltage) and to investigate properties inside the biofilm. But for a given current efficiency (how much of the current is used to make acetate) and for an imposed current, it is not necessary to set up a model for the biofilm.

2.1. Ion transport in ion-exchange membranes

Diffusion and electromigration of ions through an IEM are described by the Nernst-Planck equation

$$J_i = -D_{\mathrm{m,i}} \cdot \left(\frac{\partial c_{\mathrm{m,i}}}{\partial x} + z_i c_{\mathrm{m,i}} \frac{\partial \phi}{\partial x} \right) \tag{1}$$

where subscript i refers to ion type i, J_i is the ionic flux (mol/m^2/s), $D_{\mathrm{m},i}$ the diffusion coefficient in the membrane (m^2/s), $c_{\mathrm{m,i}}$ is the ion concentration per volume aqueous phase in the membrane (mol/m^3), x is the position coordinate in the membrane, z_i is the ion valency (e.g., +1 for Na^+), and ϕ is the dimensionless electrical potential, which can be multiplied by the thermal voltage, $V_T = RT/F$, with R the gas constant (J/mol/K), T temperature (K), and F Faraday's constant (C/mol), to obtain the voltage with dimension V. The diffusion coefficient in the membrane is a certain fraction d_f of the value in free (dilute) solution, $D_{\mathrm{aq},i}$, and the value is the same for all ions. We neglect in Eq. (1) a possible advection of ions due to volumetric (water) flow through the IEMs [26].

At each position in the membrane, mass conversation of every species is given by

$$\frac{\partial c_{\mathrm{m,i}}}{\partial t} = -\frac{\partial J_i}{\partial x} + \Gamma_i \tag{2}$$

with t time (s) and Γ_i the chemical formation rate of species i (mol/m^3/s) because of acid-base reactions. Note that in our theoretical framework Γ_i does not need to be evaluated as we will

[1] We use the terminology of protons (H^+) and hydronium ions (H_3O^+) interchangeably.

discuss below. Making the assumption of local steady-state in the membrane, the accumulation term, $\partial c_{m,i}/\partial t$, can be set to zero.

The reaction-terms, Γ_i, are dealt with as follows. For the inert anions Cl^- and cations Na^+, Eq. (2) is used with Γ_i set to zero. For all ions that undergo acid-base reactions, Eq. (2) is analysed per group of ions, in such a way that Γ_i disappears. (Note that this part of the analysis is valid irrespective of the kinetic rate of the reaction, fast or slow.) In our system, three groups are considered: a, c, and s. Group a consists of HAc and Ac^-, which are in equilibrium according to $HAc \rightleftarrows Ac^- + H^+$. Group c consists of H_2CO_3, HCO_3^- and CO_3^{2-}, which are in equilibrium according to $H_2CO_3 \rightleftarrows HCO_3^- + H^+$ and $HCO_3^- \rightleftarrows CO_3^{2-} + H^+$. Group s consists of HSO_4^- and SO_4^{2-}, which are in equilibrium according to $HSO_4^- \rightleftarrows SO_4^{2-} + H^+$. As we will discuss below, for the "water ions", H^+ and OH^-, a balance such as Eq. (2) does not need to be set up but instead the more intuitive charge balance is used, which is Eq. (4) below.

How does Γ_i cancel out for each group of ions? Let us illustrate this by deriving a mass balance for group a. Independent of kinetics, at every moment and every position, the formation of HAc is equal to the consumption of Ac^-, i.e., $\Gamma_{HAc} + \Gamma_{Ac^-} = 0$, and we can sum Eq. (2) over HAc and Ac^-, to derive a mass balance for group a where the production terms, Γ_i, cancel out. The combined mass balance becomes

$$\frac{\partial\left([HAc]_m + \left[Ac^-\right]_m\right)}{\partial t} = -\frac{\partial J_{HAc}}{\partial x} - \frac{\partial J_{Ac^-}}{\partial x}, \tag{3}$$

and in steady-state each side of this equation is zero. Note that in this work we use both the notation [..] and the symbol c_i to describe concentrations.

For group c, we use a similar approach, but with three ionic species, and we consider two chemical equilibria. In this case, the net formation of CO_3^{2-}, HCO_3^- and H_2CO_3 is zero, thus $\Gamma_{H_2CO_3} + \Gamma_{HCO_3^-} + \Gamma_{CO_3^{2-}} = 0$. To derive a mass balance for group c where the production terms, Γ_i, cancel out, we sum Eq. (2) over H_2CO_3, HCO_3^-, and CO_3^{2-}.

A similar balance describes how the local ionic charge density does not change in time,

$$\frac{\partial}{\partial t}\sum_i z_i c_{m,i} = -\frac{\partial}{\partial x}\sum_i z_i J_i \tag{4}$$

where the summation runs over all ions, including H^+ and OH^-. Eq. (4) follows from Eq. (2) when we sum over all ions and multiply by their valency z_i. The reaction term $\sum_i z_i \Gamma_i$ is zero because no (ionic) charge is produced in the acid-base reactions. Please note that, for modeling of porous electrodes, or membranes of which the fixed membrane charge, ωX, is not fixed but depends on local ion concentrations, Eq. (4) does not follow automatically [27]. Because charge cannot accumulate, each side in this equation is zero. This is correct in a dynamic calculation, as well as for steady-state.

Related, at each position in the membrane, local electroneutrality holds [20],

$$\sum_i z_i c_{m,i} + \omega X = 0 \tag{5}$$

where ω is the sign of the membrane charge (+1 for an AEM and −1 for a CEM) and X is the membrane charge expressed in moles of fixed charges (a strictly positive quantity) per unit aqueous phase in the membrane [28]. Again, the summation over i includes all ions present in the system.

Next we set up expressions for the ion fluxes and ionic current across a membrane. As the membrane is described in steady state, ion transport is constant across the membrane for the unreactive species, Na^+ and Cl^-. For these species, to calculate the ion fluxes across the membrane, we combine Eqs. (1) and (2), integrate across the membrane, and arrive at

$$J_i = -\frac{D_{m,i}}{L_m}\cdot\left(c_{m,1,i} - c_{m,0,i} + z_i\int_{\phi_0}^{\phi_1} c_{m,i}\mathrm{d}\phi\right) \tag{6}$$

where subscripts "0" and "1" refer to the very left and very right sides, just in the membrane, and where L_m is the membrane thickness. A detailed derivation of Eq. (6) can be found in Appendix A of Dykstra et al. [27] and in Biesheuvel and Dykstra [29].

For the ion fluxes of the three acid-base groups we have on the basis of Eq. (3), taking the group of $HAc + Ac^-$ as an example,

$$J_{HAc+Ac^-} = \sum_{HAc,Ac^-} \mathrm{rhs(Eq.\ (6))}. \tag{7}$$

For the ionic current density, similarly,

$$J_{charge,ionic} = \sum_i z_i \cdot \mathrm{rhs(Eq.\ (6))} \tag{8}$$

where the summation runs over all ions, including H^+ and OH^-. The ionic current density in each of the membranes, and also across each solution phase relates to the externally imposed current to the cell I (in A/m^2) by

$$I = F\cdot J_{charge,ionic}. \tag{9}$$

To calculate the transport number, T_i, which is the contribution of the flux of an ion to the local current, for each ion, we use the ion fluxes as given by Eq. (6) [29]

$$T_i = z_i\cdot J_i\cdot F/I. \tag{10}$$

The above equations are solved jointly with the acid-base equilibria that are established in our system within each group of species (such as the group that consists of HAc and Ac^-),

$$K_a = \frac{\left[Ac^-\right][H^+]}{[HAc]},\ K_{c1} = \frac{\left[HCO_3^-\right][H^+]}{[H_2CO_3]},\ K_{c2} = \frac{\left[CO_3^{2-}\right][H^+]}{\left[HCO_3^-\right]},$$
$$K_s = \frac{\left[SO_4^{2-}\right][H^+]}{\left[HSO_4^-\right]},\ K_w = \left[OH^-\right]\left[H^+\right] \tag{11}$$

which are all evaluated at each position in the membrane. The numerical values of the equilibrium constants are given in Table 1.

For all ions (charged or not) we have at the two membrane outer surfaces (positions "0" and "1" of each membrane)

$$c_{m,i} = c_{\infty,i}\cdot\exp(-z_i\cdot\Delta\phi_D) \tag{12}$$

where subscript ∞ refers to the concentration in solution, i.e., outside the membrane, and where $\Delta\phi_D$ is the Donnan potential, i.e. the potential just inside the membrane, minus that in solution [28,30].

2.2. Mass balances in solution

Considering the example cell configuration of Fig. 1, in each of the three bulk solutions (anolyte, extraction compartment, catholyte; k =a,e,c), we have the following balances for each ion

$$V_k\cdot\frac{\partial c_{k,i}}{\partial t} = A\cdot\sum_j J_{k,j,i} + V_k\cdot\Gamma_{k,i} \tag{13}$$

where $\sum_j$ refers to the fluxes through the membranes and fluxes due to electrode reactions, to be discussed below. Here, A is the area of one membrane (i.e., the cross-area of the compartment, or cell) and V_k the volume of each compartment. The volume of each compartment can be larger than the space between membranes, when the solution is pumped into/out of the cell from a storage vessel [3]. Eq. (13) assumes these volumes do not change in time; thus we neglect fluid transport through the membranes, even though this electro-osmotic flow can be significant [26,29].

Table 1
System and electrode dimensions, operational parameters, parameters used for theoretical calculations. Parameters obtained from *1) Gildemyn et al. [3] ; *2) Dykstra et al. [12] ; *3) Stumm and Morgan [31]. Initial concentrations of ionic species are reported in S.I. Table 1.

Experimental and general model parameters			
A_{cell}	Electrode geometric surface area	100	cm^2
T	Temperature	298	K
V_k	Volume anolyte, catholyte and extraction compartment *1	350	cm^3
p_{CO_2}	Partial pressure of CO_2 in gas purged through catholyte *1	0.1	bar
K_{H,CO_2}	Henry coefficient of CO_2 *2	33.46	mM/bar
I	Current density *1	5.0	A/m^2
CE	Coulombic efficiency *1	0.61	
Membrane parameters			
$L_{m,AEM}$	AEM thickness	100	µm
$L_{m,CEM}$	CEM thickness	100	µm
$L_{m,BPM}$	BPM thickness	200	µm
$d_{r,m,AEM}$	Diffusion coefficient in AEM relative to value in solution	0.050	
$d_{r,m,CEM}$	Diffusion coefficient in CEM relative to value in solution		
	in a 3-compartment cell (Figs. 2 and 3)	0.035	
	in a 2-compartment cell (Figs. 4 and 5)	0.1	
$d_{r,m,BPM}$	Diffusion coefficient in BPM relative to value in solution	0.1	
ω_{AEM}	Sign of the fixed charge AEM	+1	
ω_{CEM}	Sign of the fixed charge CEM	−1	
X_{AEM}	Fixed charge density AEM	4	M
X_{CEM}	Fixed charge density CEM	4	M
Diffusion coefficients in solution			
i		D_i ($\cdot 10^{-9}$ m^2/s) *2	
Na^+	Sodium ion	1.33	
Cl^-	Chloride ion	2.02	
HAc	Acetic acid ion	1.21	
Ac^-	Acetate ion	1.10	
H^+	Protons	9.13	
OH^-	Hydroxyl ion	5.16	
H_2CO_3	Carbonic acid ion	1.92	
HCO_3^-	Bicarbonate ion	1.18	
CO_3^{2-}	Carbonate ion	0.98	
HSO_4^-	Bisulphate ion	1.385	
SO_4^{2-}	Sulphate ion	1.065	
Listed inflow concentrations are calculated considering conditions given by Eqs. (11) and (15) and $pH_{inflow} = 3 - \log_{10}(c_{inflow,H^+})$. Furthermore, we relate c_{inflow,H_2CO_3} to the partial gas pressure of CO_2, p_{CO_2}, according to Henry's law, $c_{inflow,H_2CO_3} = K_{H,CO_2} \cdot p_{CO_2}$, where K_H is Henry's coefficient.			
Equilibrium constants of the acid-base reactions in solution *3			
$pK_{a,AC}$	$CH_3COOH \rightleftarrows CH_3COO^- + H^+$, $K_{a,AC} = \frac{[CH_3COO^-][H^+]}{[CH_3COOH]}$	4.76	
$pK_{a,CA1}$	$H_2CO_3 \leftrightarrow HCO_3^- + H^+$, $K_{a,CA1} = \frac{[HCO_3^-][H^+]}{[H_2CO_3]}$	6.35	
$pK_{a,CA2}$	$HCO_{3-} \rightleftarrows CO_3^{2-} + H^+$, $K_{a,CA2} = \frac{[CO_3^{2-}][H^+]}{[HCO_3^-]}$	10.33	
$pK_{a,S}$	$HSO_4^- \leftrightarrow SO_4^{2-} + H^+$, $K_{a,S} = \frac{[SO_4^{2-}][H^+]}{[HSO_4^-]}$	1.92	
pK_w	$H_2O \leftrightarrow H^+ + OH^-$, $K_w = [H^+][OH^-]$	14.00	
The pK_a and pK_w relate to K_a and K_w using $\log_{10}(K_a) = 3 - pK_a$ and $\log_{10}(K_w) = 6 - pK_w$.			

Eq. (13) is evaluated in this form for Na^+ and Cl^- (with $\Gamma_{k,i} = 0$), while for the ions in the "a", "c", and "s"-groups the modified form (taking HAc^+ Ac^- as example) becomes

$$V_k \cdot \frac{\partial\left([HAc]_k + \left[Ac^-\right]_k\right)}{\partial t} = A \cdot \sum_j \sum_i J_{k,j,i} \tag{14}$$

where subscript i indicates a summation over the ions within a certain group (e.g., for the "a"-group, these are HAc and Ac^-), and j is a summation over the fluxes through the membranes or electrodes (to be discussed below for each compartment), while k refers to the compartment. Eq. (14) is implemented for each group of species, and for each solution phase (k =a,e,c). Exceptions are for the carbonic acid ions (the "c"-group), for which Eq. (14) is only solved in the anolyte, and not in the other compartments because there the concentration of H_2CO_3 is fixed because CO_2-gas is bubbled through these compartments.

In each of the three compartments, Eqs. (13) and (14) are supplemented by the condition of electroneutrality, which we considered in the membranes as well (Eq. (5)),

$$\sum_i z_i c_{k,i} = 0. \tag{15}$$

As a next step, in each compartment mass balance, Eq. (13), two boundary fluxes $J_{j,i}$ must be implemented. First of all there are the fluxes through the membranes, as described by Eqs. (6) and (7). Note that each membrane flux will show up in two compartment balances, once as a positive contribution, once negative. Making use of the coordinate system as in Fig. 1, where the coordinate x-axis runs from left to right (and thus fluxes J_i defined positive towards the right), then a (membrane) flux entering the compartment on the lhs is taken as a positive contribution ("with a plus-sign") and a flux leaving on the rhs is implemented as a negative contribution ("with minus sign"). Secondly, there are contributions due to the electrode reactions, as explained in the next section.

For the extraction and catholyte compartments, the partial pressure of the gas CO_2 that is bubbled through the catholyte, p_{CO_2}, relates to the concentration in solution of carbonic acid,

H_2CO_3, according to Henry's law

$$[H_2CO_3] = K_{H,c} \cdot p_{CO_2} \tag{16}$$

with $K_{H,c}$ Henry's coefficient for CO_2-adsorption ($K_{H,c} = 33.46$ mM/bar). For H_2CO_3, we assume that the chemical reaction between unhydrated CO_2 and hydrated H_2CO_3 in water is infinitely fast.

2.3. Electrode reactions

In the next section we explain the two remaining fluxes for the ions, due to the electrode reactions on the two electrodes. For the inert species Na^+ and Cl^- we simply have a zero reaction flux at the electrode, and the same goes for the group SO_4^{2-} + HSO_4^-, as there is no formation of these species at the electrode. Thus in the mass balances for the anolyte and catholyte compartment for Na^+, Cl^-, and for the "s"-group, only the membrane flux is required.

This only leaves us to discuss how the reactions impact the balances for the "c"- and "a"-groups. Note first of all, we do not need to consider which ion is involved in an electrode reaction, e.g., whether it is HAc or Ac^- that is formed, is of no concern. Instead, the theory self-consistently calculates in which form the species is present in each compartment. Note also, again, that OH^- and H^+ do not need to be explicitly considered in relating electrode reaction rates to the current, as illustrated next.

First, let us consider the anode. Here, water reacts to protons and oxygen (gas). Or, equivalently, OH^--ions react to O_2 and water. From the point of reaction stoichiometry, both reactions are equivalent. In any case, with this reaction on the anode, there is no involvement of either the "c"- or "a"-groups. So for these two groups, the reaction flux J_i is zero in the anolyte, and thus the reaction of oxygen formation does not show up explicitly in any of the mass balances.

Second, we consider the cathode. Let us discuss how the various fluxes are linked to one another, and linked to the electrical current. Assuming the reaction of acetate from carbonate to be the only electrode reaction taking place, we can relate the consumption/production flux of ions in each group to the electronic current, I (in A/m^2), because we know that for each carbonate ion that reacts away (irrespective of whether it is H_2CO_3, HCO_3^- or CO_3^{2-}), four electrons enter into solution (from the electrode), while for each two carbonate ions that disappear one acetate ion is formed (again, irrespective of which ion from a group). This is quantified as

$$I/F \cdot \mathrm{CE} = 4 \cdot J^e_{H_2CO_3+HCO_3^-+CO_3^{2-}} = -8 \cdot J^e_{HAc+Ac^-} \tag{17}$$

where superscripts e are implemented to distinguish this electrode flux from the membrane fluxes that are described by Eqs. (6) and (7). In the ideal case just discussed, all electronic current is used to convert carbonate into acetate, and thus the Coulombic efficiency, CE, is unity (CE = 1). However, often also other reactions take place, involving water and the H^+ and OH^- ions (or other ions), which implies the Coulombic efficiency is less than unity. This is also the case in the calculations in this paper. If no other electrode reactions are considered but the carbonate to acetate reaction discussed above, and if CE is some number less than unity, this implies that the remainder of the electronic current is involved in a reaction with water, H^+ and/or OH^-. This reaction involving water, H^+, and OH^-, similar to the reactions on the anode, does not need to be explicitly considered in the numerical calculations, but nevertheless they affect the calculation outcome, such as pH in the catholyte compartment, i.e., this reaction is most certainly part of the physical description of this problem.

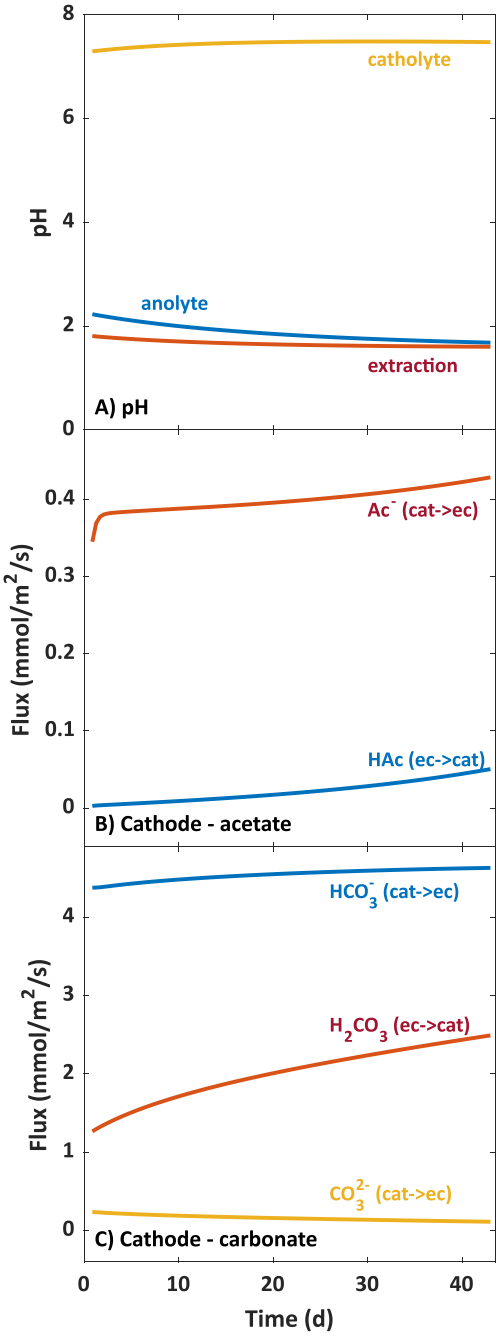

Fig. 3. Theory of pH in anolyte, extraction compartment and catholyte in a 3-compartment electrosynthesis cell as depicted in Fig. 1 (a). Transport of Ac^- from the catholyte *(cat)* to the extraction compartment *(ec)* and of HAc from the *ec* to *cat* (b), and transport of HCO_3^- and CO_3^{2-} from *cat* to *ec*, and of H_2CO_3 from *ec* to *cat* (c). Fluxes are evaluated in the membrane at the point where it faces the catholyte compartment. Inputs for the theoretical calculations are the same as in Fig. 2 and are summarized in Table 1.

3. Results and discussion

3.1. Acetate production and recovery

In the first calculation, we consider the three-compartment MES cell discussed by Gildemyn et al. [3], and we use the parameter values listed in Table 1. The measured and calculated production rates of acetate in the extraction compartment, anolyte, and catholyte, are shown in Fig. 2. 'Acetate' in this context refers the sum of HAc and Ac^-.

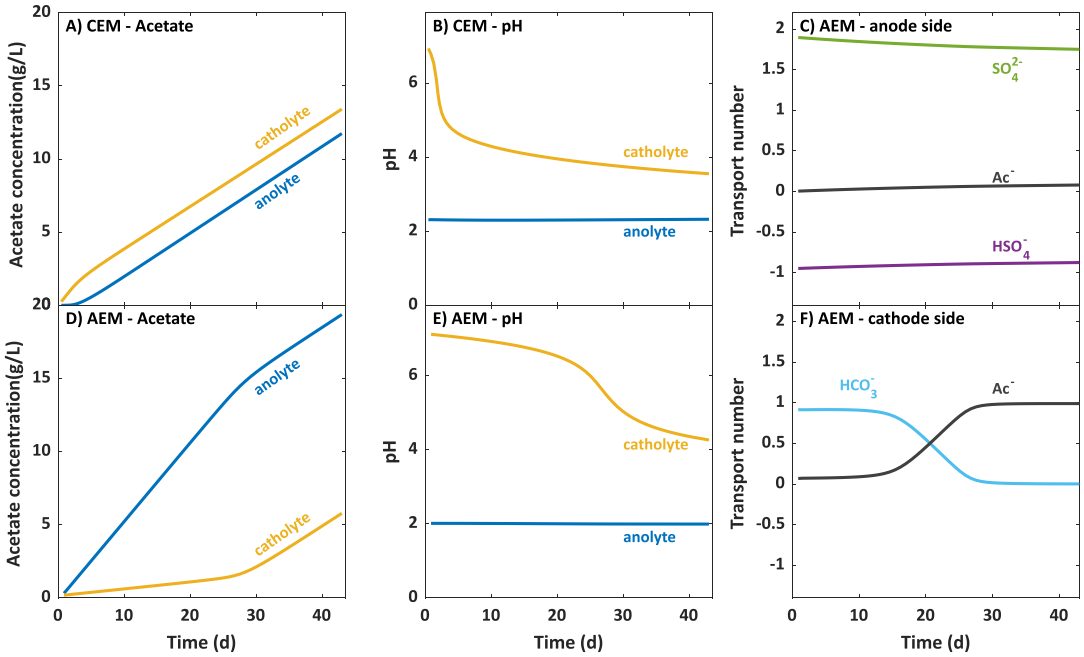

Fig. 4. Theory of acetate concentration (a,d) and pH (b,e) in the anolyte and catholyte in a two-compartment cell with only a cation exchange membrane (a,b) or only an anion exchange membrane (d,e). Transport numbers with only an anion exchange membrane are evaluated in the membrane at the anode side (c) and at the cathode side (f). For cations, a positive transport number implies the ion flows from anode to cathode, while for anions a positive transport number implies the reverse. In a cation exchange membrane, the transport number of H^+ is equal to 1, and of all other ions close to 0 (not shown).

Gildemyn et al. [3] shows that the highest acetate concentration is obtained in the extraction compartment. In the catholyte, the acetate concentration increases and reaches a stable value, while in the anolyte the acetate concentration continuously increases with time. The theory (Fig. 2B) shows similar trends, such as that the highest acetate concentration is obtained in the extraction compartment. The anolyte concentration of acetate is close to that in the extraction compartment, while the concentration in the catholyte increases at a much lower rate.

3.2. Acetate transport across the membranes

The theory allows for detailed analysis of transport of acetate and other ions across the membranes. As shown in Fig. 3, pH as function of time is quite stable in all three compartments, with the catholyte pH stabilizing around pH 7.5, while in the anolyte pH = 1.6, and in the recovery compartment pH = 1.7. Gildemyn et al. [3] reported a pH of 1.7 in the extraction compartment, in agreement with the calculated pH, though catholyte pH was reported as pH 8.4, somewhat higher than the value we calculate.

Ac^- transport from the catholyte to the extraction compartment increases slightly over time (Fig. 3). This Ac^- transport to the extraction compartment is considerably higher than the transport of HAc from the extraction compartment back to the catholyte. This so-called backtransport is undesired, as it results in a lower extraction efficiency. It is a combined effect of the increasing acetate concentration and decrease in pH in the extraction compartment, resulting in a larger driving force for HAc diffusion from the extraction compartment to the catholyte. The transport number for Ac^- was around 7% which corresponds well to the reported transport number of 8.1% [3].

In addition to Ac^- transport, also transport of other ions can be analyzed with the theory. Transport of HCO_3^- from the catholyte to the extraction compartment was roughly 10 times higher than Ac^- transport, implying that large part of the fed CO_2 is transported away from the catholyte. At the same time, HCO_3^- is protonated in the extraction compartment where pH is low, and there is transport of H_2CO_3 from extraction compartment back to catholyte. Thus, part of the transported HCO_3^- is recycled to the catholyte as H_2CO_3. Transport numbers of HCO_3^- and other anions across the AEM were not analyzed in the experimental work, but the authors suggested that HCO_3^-, Cl^- and OH^- were the main other charge carriers. Our calculations show that HCO_3^- accounted for 78-81% of the transported charge, which implies that compared to Ac^-, 11 times more charge was carried by HCO_3^-. The remainder of the current was carried by CO_3^{2-} (up to 8%), while Cl^- accounted for ~1%. Transport of OH^- was negligible. In addition, the calculated results show that SO_4^{2-} is transported from the extraction compartment to the catholyte (transport number of -3%).

We make additional calculations for a simplified electrochemical cell design. Fig. 4 illustrates a simplified process when only a cation exchange membrane (CEM) or only an anion exchange membrane (AEM) is used. If only an AEM is used, the acetate concentrations in the anolyte and catholyte have similar trends (Fig. 4D) compared to the original situation (Fig. 2) in the three-compartment cell. Instead, if only a CEM is used, the theory predicts a very strong decrease of the pH in the catholyte, and the pH is much lower than in the three-compartment cell. Interestingly, also [4] observed a lower value of the catholyte pH during the experiments when only a CEM was used, and they had to maintain the pH around 6.6 by regularly dosing a 1 M NaOH solution.

Fig. 4 also shows the transport numbers of various ionic species across the AEM, evaluated in the membrane at the anode side (Fig. 4C) and at the cathode side (Fig. 4F). In case an AEM is used, many amphoteric ions contribute to charge transport, and the contribution is different at both sides of the membrane. What can be observed is that, at the anode side, charge is mainly carried by HSO_4^- and SO_4^{2-} ions, and the contribution of these ions is more or less constant over time, with HSO_4^- on this side entering the membrane and SO_4^{2-} leaving the membrane. At the cathode side, HCO_3^- plays a role at the start of the experiment, but after ~25 days the contribution of HCO_3^- is completely taken over by Ac^-.

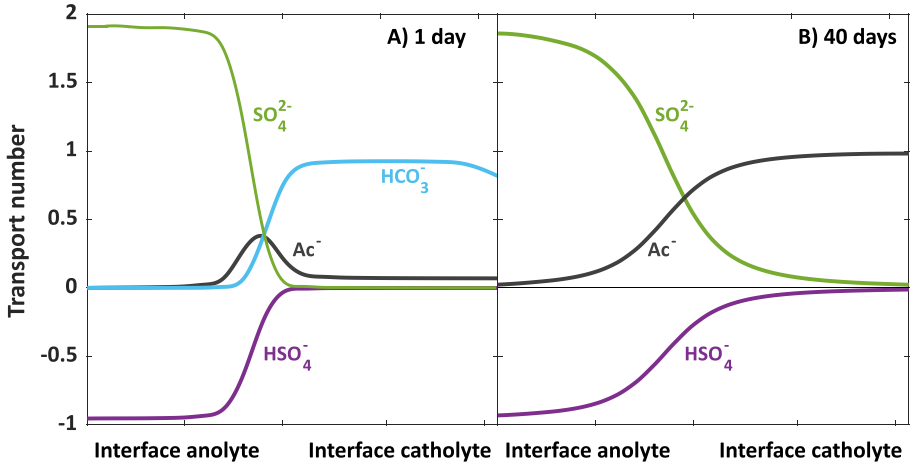

Fig. 5. Transport numbers in a two-compartment cell with an anion exchange membrane as function of position in the membrane, a) after 1 day of operation and b) after 40 days of operation. Transport numbers of ionic species with values close to zero are not shown. Concentrations of ionic species in both compartments are reported in S.I. Table 2.

We furthermore find that in case a CEM is used, the current is completely transported by protons (not shown). Also H_2CO_3 and HAc are transported across the membrane, see Fig. 4, but because they are uncharged, their transport number is zero.

As we discussed in de Lichtervelde et al. [14] the ionic current is mainly carried by the group of ionic species with a pK value closest to the pH at that position. Thus, where pH is close to $pK_{a,CA1} = 6.4$, current is mainly carried by the H_2CO_3 and HCO_3^- ions, and where pH is close to $pK_{a,AC} = 4.8$, it is the HAc and Ac^- ions. Finally, when pH is close to $pK_{a,S} = 1.9$, current is transported by the HSO_4^- and SO_4^{2-} ions. Thus we observe that at the anode side where pH ~ 2, the group of sulphate ions carries the current. At the cathode side, during the first 20 days of the experiment, the pH is much higher (> 6), and therefore the group of bicarbonate ions carries the current. When the current decreases (after approx. 20 days), the group of acetate ions takes over.

Fig. 5 shows transport numbers in a two-compartment cell with an AEM after 1 day and 45 days of operation as function of position. At the membrane-anolyte interface current is carried by the HSO_4^- and SO_4^{2-} ions. However, at the membrane-catholyte interface, it is transported by HCO_3^- at the start of the experiment, when the pH in the catholyte is still above pH 6, while after 40 days of operation, when the pH decreased to values close to pH 4, this role is taken over by Ac^-.

3.3. Bipolar membrane

A bipolar membrane (BPM) can be theoretically described as an AEM and CEM in direct contact, with a vanishingly thin aqueous layer in between. Thus we have an AEL and CEL (with L for 'layer') that together form a BPM. The cell configuration is the same as the three-compartment cell illustrated in Fig. 1, but with a vanishingly small aqueous region between the two membrane layers. In the present case, with a BPM, another modification is made to Fig. 1: the AEL is positioned towards the anode, and the CEL towards the cathode. All membrane parameter values are reported in Table 1.

Fig. 6 shows the predicted development of concentrations of ions as function of time in the anolyte and catholyte. Acetate is produced at the cathode, and because of the low pH (close to or below pH 5 after 10 days of operation), part of the acetate is converted to its uncharged form, which is transported through the BPM to the anolyte by diffusional forces. Furthermore, Fig. 6D shows a distinct decrease of pH in the catholyte, which is in line with experimental findings by [4], who found a pH decrease in the catholyte when a BPM was used in the same way as in our theoretical model.

Moreover, we analyzed the transport numbers across the AEL and CEL (results not shown). These transport numbers are evaluated on the outside interfaces of the membrane (just inside the membrane). We find that the current is completely carried by protons in the CEL. In the AEL, the current is mainly carried by the HSO_4^- and SO_4^{2-} ions, with $pK_{a,S} = 1.92$, and this and this is due to the low pH in the anolyte. We find a negative value for the transport number of HSO_4^- ($T_i = -0.94$), while the transport number of SO_4^{2-} is higher than 1 ($T_i = 1.88$). These numbers imply SO_4^{2-} flows from the anode through the AEL to the interface with the CEL, while HSO_4^- flows in reverse direction. We note that the summation of the transport numbers of all ions in the membranes is always equal to $\sum_i T_i = 1$. Based on these findings, we conclude that a frequently made assumption about BPMs, namely that current is predominantly carried by H^+ and OH^-, that are produced at the interface between AEL and CEL, is not correct if amphoteric ions are present. According to our calculation, it is correct that H^+ is produced in acid-base reactions at the interface, but OH^- is not produced as a species that then flows through the AEL. Instead, other anions carry the current in the AEL. Thus, in order to describe and explain ion transport in BPMs, all ionic species have to be considered, especially the amphoteric ions.

4. Conclusions

In this work we have set up a dynamic one-dimensional theoretical framework to describe the transport of the amphoteric ions which participate in acid-base reactions and across (bipolar) ion exchange membranes (BPMs). The theory is applied to the case of a microbial electrosynthesis cell, which converts CO_2 into acetate. The theory includes reactions at the electrodes.

In this theoretical approach all fluxes are self-consistently calculated without prescribing any of the fluxes. The theory does not require that one defines the fluxes of H^+ or OH^- at the electrodes, and neither do we have to define whether acetate (Ac^-) or acetic acid (HAc) is produced at the electrode, or which carbonate ions (H_2CO_3, HCO_3^- or CO_3^{2-}) is consumed. Lastly, to theoretically describe a bipolar membrane, we do not have to make the common assumption that ionic charge is only carried by H^+ and OH^-.

As an example calculation, we considered the three-compartment MES cell of Gildemyn et al. [3]. The theory describes the general trends observed experimentally. Furthermore, our

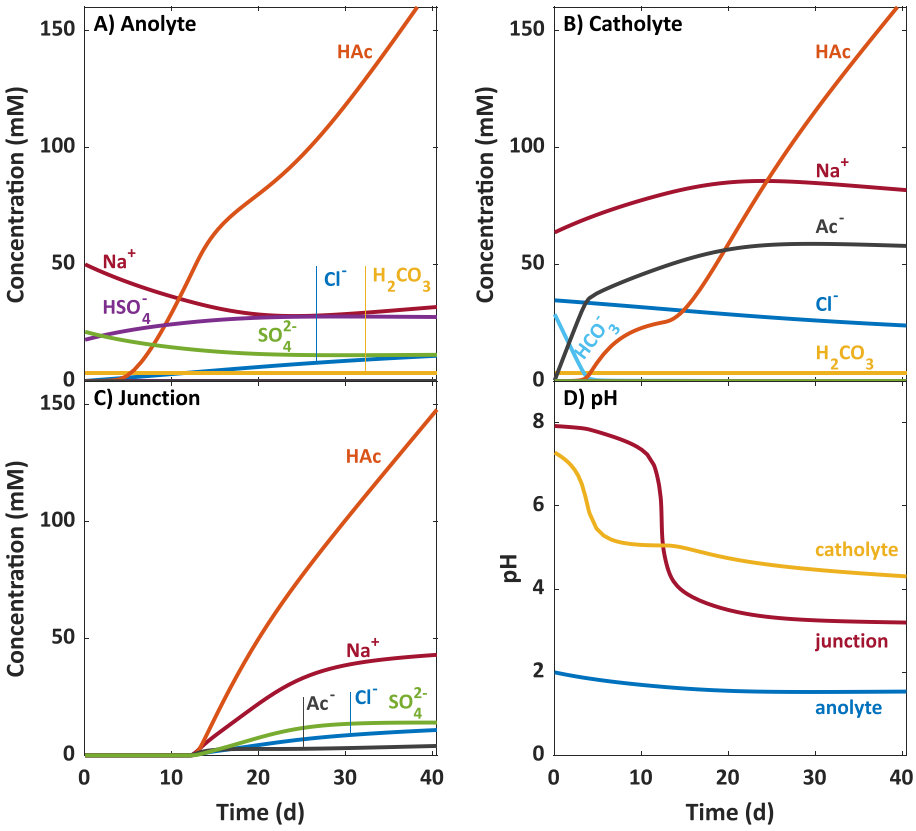

Fig. 6. Theory of transport of amphoteric ions across a bipolar membrane, with the anion exchange layer positioned towards the anode, and the cation exchange layer towards the cathode. (a) Ion concentrations in anolyte, and (b) catholyte, and (c) at the interface between the cation and anion exchange layers. (d) pH in anolyte and catholyte, and at the interface.

results show that a commonly made assumption that in BPMs the current is carried by H^+ and OH^-, and that these species are produced at the interface between the anion-exhange layer and cation-exchange layer, is not correct. We find that, in order to describe and explain ion transport in BPMs, amphoteric ionic species have to be considered. These amphoteric ions, for example HSO_4^-, can carry a proton across the anion exchange layer of the BPM to the interface with the cation exchange layer, and this bisulphate ion is thereafter transported in the reverse direction in unprotonated form, as SO_4^{2-}.

Declaration of competing interest

The authors declare that they have no known competing financial interests or personal relationships that could have appeared to influence the work reported in this paper.

Acknowledgements

The authors thank prof.dr.ir. Korneel Rabaey for fruitful discussions regarding the experimental findings of their microbial electrosynthesis cells. A.t.H. acknowledges funding by the research program Vidi (with project number 17516), which is (partly) financed by the Dutch Research Council (NWO). S.P. is a Serra Húnter Fellow (UdG-AG-575) and acknowledges funding from the ICREA Acadȩmia award and the Spanish Ministry of Science (RTI2018-098360-B-I00). LEQUiA has been recognized as consolidated research group by the Catalan Government with code 2017-SGR-1552.

References

[1] I. Vassilev, P.A. Hernandez, P. Batlle-Vilanova, S. Freguia, J.O. Krömer, J. Keller, P. Ledezma, B. Virdis, Microbial electrosynthesis of isobutyric, butyric, caproic acids, and corresponding alcohols from carbon dioxide, ACS Sustainable Chemistry and Engineering 6 (7) (2018) 8485–8493, doi:10.1021/acssuschemeng.8b00739.

[2] A. Prévoteau, J.M. Carvajal-Arroyo, R. Ganigué, K. Rabaey, Microbial electrosynthesis from CO_2: forever a promise? Curr. Opin. Biotechnol. 62 (2020) 48–57, doi:10.1016/j.copbio.2019.08.014.

[3] S. Gildemyn, K. Verbeeck, R. Slabbinck, S.J. Andersen, A. Prévoteau, K. Rabaey, Integrated production, extraction, and concentration of acetic acid from CO_2 through microbial electrosynthesis, Environ. Sci. Technol. Lett. 2 (2015) 325–328, doi:10.1021/acs.estlett.5b00212.

[4] S. Gildemyn, R.A. Rozendal, K. Rabaey, A gibbs free energy-Based assessment of microbial electrocatalysis, Trends Biotechnol. 35 (2017) 393–406, doi:10.1016/j.tibtech.2017.02.005.

[5] L. Jourdin, S. Freguia, B.C. Donose, J. Chen, G.G. Wallace, J. Keller, V. Flexer, A novel carbon nanotube modified scaffold as an efficient biocathode material for improved microbial electrosynthesis, Journal of Materials Chemistry A 2 (2014) 13093–13102, doi:10.1039/c4ta03101f.

[6] F. Kracke, A.B. Wong, K. Maegaard, J.S. Deutzmann, M.K. Hubert, C. Hahn, T.F. Jaramillo, A.M. Spormann, Robust and biocompatible catalysts for efficient hydrogen-driven microbial electrosynthesis, Communications Chemistry 2 (2019) 1–9, doi:10.1038/s42004-019-0145-0.

[7] P. Batlle-Vilanova, S. Puig, R. Gonzalez-Olmos, M.D. Balaguer, J. Colprim, Continuous acetate production through microbial electrosynthesis from CO_2 with microbial mixed culture, J. Chem. Technol. Biotechnol. 91 (2016) 921–927, doi:10.1002/jctb.4657.

[8] L. Jourdin, Y. Lu, V. Flexer, J. Keller, S. Freguia, Biologically induced hydrogen production drives high rate/high efficiency microbial electrosynthesis of acetate from carbon dioxide, ChemElectroChem 3 (2016) 581–591, doi:10.1002/celc.201500530.

[9] R. Blasco-Gómez, S. Ramió-Pujol, L. Bañeras, J. Colprim, M.D. Balaguer, S. Puig, Unravelling the factors that influence the bio-electrorecycling of carbon dioxide towards biofuels, Green Chem. 21 (3) (2019) 684–691, doi:10.1039/c8gc03417f.

[10] B. Korth, F. Harnisch, Modeling Microbial Electrosynthesis, Advances in Biochemical Engineering/Biotechnology, 2017.

[11] F. Matemadombo, S. Puig, R. Ganigué, R. Ramírez-García, P. Batlle-Vilanova, M. Dolors Balaguer, J. Colprim, Modelling the simultaneous production and separation of acetic acid from CO_2 using an anion exchange membrane microbial electrosynthesis system, J. Chem. Technol. Biotechnol. 92 (2017) 1211–1217, doi:10.1002/jctb.5110.
[12] J.E. Dykstra, P.M. Biesheuvel, H. Bruning, A. ter Heijne, Theory of ion transport with fast acid-base equilibrations in bioelectrochemical systems, Physical Review E 90 (2014) 013302, doi:10.1103/PhysRevE.90.013302.
[13] J.M. Paz-Garcia, J.E. Dykstra, P.M. Biesheuvel, H.V.M. Hamelers, Energy from CO_2 using capacitive electrodes a model for energy extraction cycles, J. Colloid Interface Sci. 442 (2015) 103–109, doi:10.1016/j.jcis.2014.11.045.
[14] A.C.L. de Lichtervelde, A. ter Heijne, H.V.M. Hamelers, P.M. Biesheuvel, J.E. Dykstra, Theory of ion and electron transport coupled with biochemical conversions in an electroactive biofilm, Phys. Rev. Appl. 12 (2019) 014018, doi:10.1103/PhysRevApplied.12.014018.
[15] S. Mareev, E. Evdochenko, M. Wessling, O. Kozaderova, S. Niftaliev, N. Pismenskaya, V. Nikonenko, A comprehensive mathematical model of water splitting in bipolar membranes: impact of the spatial distribution of fixed charges and catalyst at bipolar junction, J. Memb. Sci. 603 (2020) 118010, doi:10.1016/j.memsci.2020.118010.
[16] V. Volgin, A. Davydov, Ionic transport through ion-exchange and bipolar membranes, J. Memb. Sci. 259 (2005) 110–121, doi:10.1016/j.memsci.2005.03.010.
[17] V.I. Kovalchuk, E.K. Zholkovskij, E.V. Aksenenko, F. Gonzalez-Caballero, S.S. Dukhin, Ionic transport across bipolar membrane and adjacent nernst layers, J. Memb. Sci. 284 (1–2) (2006) 255–266, doi:10.1016/j.memsci.2006.07.038.
[18] Z. Yan, L. Zhu, Y.C. Li, R.J. Wycisk, P.N. Pintauro, M.A. Hickner, T.E. Mallouk, The balance of electric field and interfacial catalysis in promoting water dissociation in bipolar membranes, Energy & Environmental Science 11 (7) (2018) 2235–2245.
[19] D.A. Vermaas, S. Wiegman, T. Nagaki, W.A. Smith, Ion transport mechanisms in bipolar membranes for (photo)electrochemical water splitting, Sustainable Energy & Fuels 2 (2018) 2006–2015.
[20] Y.L. Hwang, F.G. Helfferich, Generalized-Model for multispecies ion-Exchange kinetics including fast reversible-Reactions, React. Polym. 5 (1987) 237–253, doi:10.1016/0167-6989(87)90233-9.
[21] M.S. Hall, V.M. Starov, D.R. Lloyd, Reverse osmosis of multicomponent electrolyte solutions. part i. theoretical development, J. Memb. Sci. 128 (1997) 23–37, doi:10.1016/S0376-7388(96)00300-6.
[22] Y.S. Oren, P.M. Biesheuvel, Theory of ion and water transport in reverse-Osmosis membranes, Phys. Rev. Appl. 9 (2) (2018) 024034, doi:10.1103/PhysRevApplied.9.024034.
[23] R. Ronen, I. Atlas, M.E. Suss, Theory of flow batteries with fast homogeneous chemical reactions, J. Electrochem. Soc. 165 (2018) A3820–A3827, doi:10.1149/2.0251816jes.
[24] D.A. Saville, O.A. Palusinski, Theory of electrophoretic separations. part i: formulation of a mathematical model, AIChE J. 32 (1986) 207–214.
[25] P.M. Biesheuvel, L. Zhang, P. Gasquet, B. Blankert, M. Elimelech, W.G.J. van der Meer, Ion selectivity in brackish water desalination by reverse osmosis: theory, measurements, and implications, Environ. Sci. Technol. Lett. 7 (2020) 42–47, doi:10.1021/acs.estlett.9b00686.
[26] M. Tedesco, H.V.M. Hamelers, P.M. Biesheuvel, Nernst-Planck transport theory for (reverse) electrodialysis: II. effect of water transport through ion-exchange membranes, J. Memb. Sci. 531 (2017) 172–182, doi:10.1016/j.memsci.2017.02.031.
[27] J.E. Dykstra, K.J. Keesman, P.M. Biesheuvel, A. van der Wal, Theory of ph changes in water desalination by capacitive deionization, Water Res. 119 (2017) 178–186, doi:10.1016/j.watres.2017.04.039.
[28] A.H. Galama, J.W. Post, M.A. Cohen Stuart, P.M. Biesheuvel, Validity of the boltzmann equation to describe donnan equilibrium at the membranesolution interface, J. Memb. Sci. 442 (2013) 131–139, doi:10.1016/j.memsci.2013.04.022.
[29] P.M. Biesheuvel, J.E. Dykstra, Physics of Electrochemical Processes, http://www.physicsofelectrochemicalprocesses.com, 2020.
[30] I. Atlas, M.E. Suss, Theory of simultaneous desalination and electricity generation via an electrodialysis cell driven by spontaneous redox reactions, Electrochim. Acta 319 (2019) 813–821, doi:10.1016/j.electacta.2019.06.014.
[31] W. Stumm, J.J. Morgan, Aquatic chemistry - Chemical equilibria and rates in natural waters, John Wiley and Sons Ltd, 1995.